

Assessment of Reinforcement Learning for Macro Placement

Chung-Kuan Cheng
University of California, San Diego
La Jolla, California, USA

Andrew B. Kahng
University of California, San Diego
La Jolla, California, USA

Sayak Kundu
University of California, San Diego
La Jolla, California, USA

Yucheng Wang
University of California, San Diego
La Jolla, California, USA

Zhiang Wang
University of California, San Diego
La Jolla, California, USA

ABSTRACT

We provide open, transparent implementation and assessment of Google Brain’s deep reinforcement learning approach to macro placement [9] and its Circuit Training (CT) implementation in GitHub [23]. We implement in open-source key “blackbox” elements of CT, and clarify discrepancies between CT and [9]. New testcases on open enablements are developed and released. We assess CT alongside multiple alternative macro placers, with all evaluation flows and related scripts public in GitHub. Our experiments also encompass academic mixed-size placement benchmarks, as well as ablation and stability studies. We comment on the impact of [9] and CT, as well as directions for future research.

CCS CONCEPTS

• **Hardware** → **Electronic design automation; Physical design (EDA); Partitioning and floorplanning.**

KEYWORDS

Macro placement, Reinforcement learning, Modern benchmarks

ACM Reference Format:

Chung-Kuan Cheng, Andrew B. Kahng, Sayak Kundu, Yucheng Wang, and Zhiang Wang. 2023. Assessment of Reinforcement Learning for Macro Placement. In *Proceedings of the 2023 International Symposium on Physical Design (ISPD ’23)*, March 26–29, 2023, Virtual Event, USA. ACM, New York, NY, USA, 9 pages. <https://doi.org/10.1145/3569052.3578926>

1 INTRODUCTION

In June 2021, authors from the Google Brain and Chip Implementation and Infrastructure (CI2) teams reported a novel reinforcement learning (RL) approach for macro placement [9] (*Nature*). The authors stated, “In under six hours, our method automatically generates chip floorplans that are superior or comparable to those produced by humans in all key metrics, including power consumption, performance and chip area.” Results were reported to be superior to those of an academic placer [3] and simulated annealing. Data and code availability was promised (“The code used to generate these data is available from the corresponding authors upon reasonable request”). Google’s Circuit Training (CT) repository [23], which

“reproduces the methodology published in the Nature 2021 paper”, was made public in January 2022.

Evaluation of *Nature* and CT has been hampered because neither data nor code in these works is, to date, fully available. A “Stronger Baselines” (SB) manuscript [11] claims that a stronger simulated annealing baseline outperforms *Nature*, but apparently uses a Google-internal version of CT along with different benchmarks and evaluation metrics. Overall, inability to reproduce *Nature* methods and results has led to controversy and slowed progress in the field.

This paper summarizes efforts toward an open-source, transparent implementation and assessment of *Nature* and CT. Results are public in the *MacroPlacement* GitHub repository [33]. Additional background and details are given in a “For the Record” series of updates [37], and in the “Our Progress” [34] and other documentation in *MacroPlacement*. Our main contributions are as follows.

- We summarize the major miscorrelations between *Nature* and CT. We also describe the reverse-engineering of key “blackbox” elements of CT – force-directed placement (Sec. 3.2.1) and proxy cost calculation (Sec. 3.2.2) – which are not clearly documented in *Nature* or open-sourced in CT. Further, we implement the grid-based Simulated Annealing macro placement that is used for comparison by both *Nature* and SB.
- We extend open foundations for academic research through (i) augmentation of SKY130HD [19] and ASAP7 [18] design enablements; (ii) bringup of modern, macro-heavy testcases including Ariane [13], BlackParrot (Quad-Core) [14] and MemPool Group [15]; and (iii) interactions with major EDA vendors leading to policy changes that permit Tcl script sharing by researchers in GitHub [12] [29].
- We assess CT using benchmarks implemented in NanGate45 [16] and GlobalFoundries GF12LP. Methods used for comparison include (i) a SOTA commercial macro placer (CMP); (ii) simulated annealing following [11] (SA); (iii) human-expert solutions; (iv) Nvidia’s AutoDMP [1]; and (v) RePlace [22]. The evaluation flows and related Tcl scripts are public in *MacroPlacement* [42]. Comparisons (ii), (iii) and (v) are also made in the *Nature* work.
- We report experimental assessments that shed light on several aspects of CT: (i) how use of initial placement information from a commercial physical synthesis tool affects CT results; (ii) stability of CT; (iii) correlation between CT’s proxy cost and “ground truth” outputs of a commercial EDA tool; and (iv) performance on ICCAD04 testcases studied in the SB manuscript.

In the following, Section 2 lists the macro placement methods studied, and Section 3 describes efforts toward open-source replication of CT. Sections 4, 5 and 6 present experimental setup and methods,

Permission to make digital or hard copies of part or all of this work for personal or classroom use is granted without fee provided that copies are not made or distributed for profit or commercial advantage and that copies bear this notice and the full citation on the first page. Copyrights for third-party components of this work must be honored. For all other uses, contact the owner/author(s).
ISPD ’23, March 26–29, 2023, Virtual Event, USA
© 2023 Copyright held by the owner/author(s).
ACM ISBN 978-1-4503-9978-4/23/03.
<https://doi.org/10.1145/3569052.3578926>

along with results using both modern and academic benchmarks. Section 7 gives conclusions and directions for future research.

2 MACRO PLACEMENT METHODS

VLSI physical design researchers and practitioners have studied macro placement for well over half a century, as reviewed in [8] [10]. We study the following macro placement methods.

- **CT** [23] uses the RL approach to place macros in sequence. CT first divides the layout canvas into small grid cells, using placement locations along with hypergraph partitioning to group standard cells into standard-cell clusters, to set up the environment. Then, the RL agent places macros one by one onto the centers of grid cells; after all macros are placed, force-directed placement is used to determine the locations of standard-cell clusters (see Sec. 3.2.1). Finally, *proxy cost* (Sec. 3.2.2) is calculated and provided as the reward feedback to the RL agent.
- **RePlace** [3] [22] models the layout and netlist as an electrostatic system. Instances are modeled as electric charges, and the density penalty as potential energy. The instances are spread according to the gradient with respect to the density penalty.
- **AutoDMP** [1] from Nvidia builds on the GPU-accelerated global placer DREAMPlace [6] and detailed placer ABCDPlace [7]. AutoDMP adds enhanced concurrent macro and standard cell placement, along with automatic parameter tuning based on multi-objective Bayesian optimization (MOBO).
- **CMP** is a state-of-the-art commercial macro placer from Cadence which performs concurrent macro and standard cell placement. CMP results also serve as input to the Cadence Genus iSpatial physical synthesis tool.
- **Human-Expert** macro placements are contributed by individuals at IBM Research [28], ETH Zurich and UCSD [30]; human-expert placements are one of the two baselines used by *Nature* authors.
- **Simulated Annealing (SA)** is a baseline used by *Nature* authors, and studied by both *Nature* and *SB*. Annealing is applied to place macros in the same grid cells as *CT* (see Sec. 3.3).

3 REPLICATION OF CIRCUIT TRAINING

We now describe clarifications and reproduction in open source of *CT*. First, we summarize the main misconceptions between *Nature* and *CT*. Second, we explain details of key “blackbox” elements of *CT*, i.e., force-directed placement and proxy cost calculation, which are to date hidden behind *plc_client* APIs in *CT*. Third, we describe our implementation of Simulated Annealing. We thank Google engineers for answering questions and for many discussions that have helped our understanding since April 2022.

3.1 Mismatches between *CT* and *Nature*

We find several significant mismatches between *CT* and *Nature*.

- *CT* assumes that all instances of the input netlist have (x, y) locations, i.e., the netlist *has already been placed* before it is input to *CT*. The location information is used by *CT*'s grouping, gridding and clustering process. However, this was not apparent during the paper review [37], and is not mentioned in *Nature* [9]. Experiments in Sec. 5.2.1 show that having initial placement information can significantly enhance *CT* outcomes.
- The proxy cost function defines the objective that drives the RL agent's learning. In Eq. 2 below, *CT* sets congestion weight λ to

0.5 and density weight γ to 1.0. *Nature* indicates “the congestion weight λ is set to 0.01, the density weight γ is set to 0.01”. However, engineers from Google Brain have suggested that we set congestion weight $\lambda = 0.5$ and density weight $\gamma = 0.5$ [27]; we follow this last suggestion in all of our experiments. Sensitivity of conclusions to the weighting of proxy cost elements is discussed in Sec. 6 below.

- *Nature* “place[s] the centre of macros and standard cell clusters onto the centre of the grid cells”. However, *CT* does not require standard-cell clusters to be placed onto centers of grid cells. (See Sec. 3.2.1.)
- *Nature* describes generation of the adjacency matrix based on the *register distance* between pairs of nodes. This is consistent with timing being a key metric for placement quality. However, *CT* builds the adjacency matrix based only on direct connections between nodes (i.e., macros, IO ports and standard-cell clusters).

3.2 Clarifying “blackbox” elements of *CT*

We now explain two key “blackbox” elements of *CT*: force-directed placement and proxy cost calculation. Neither is clearly documented in *Nature*, nor visible in *CT*. These examples are representative of the reverse-engineering needed to understand and reimplement methods that to date are visible only through APIs in the *plc_client* of [23]. Note that when performing force-directed placement and proxy cost calculation, *CT* assumes that each standard-cell cluster has a square shape.

3.2.1 Force-directed placement. Force-directed placement (**FD**) is used to place standard-cell clusters based on the *fixed* locations of macros and IO ports. During FD, only standard-cell clusters can be moved, and they are not necessarily placed onto centers of grid cells. At the start of FD, all standard-cell clusters are placed at the center of the canvas. Then, the locations of standard-cell clusters are iteratively updated. Each iteration first calculates the forces exerted on each node (macro, standard-cell cluster or IO port). There are two types of forces between nodes: *attractive* and *repulsive*.

Attractive force (F_a) applies only to pairs of nodes that are connected by nets. All multi-pin nets are decomposed into two-pin nets using the star model. For the two-pin net connecting pin $P1$ of node $M1$ and $P2$ of node $M2$, the attractive force components applied to $M1$ and $M2$ are $F_{a_x} = k_a \times \text{abs}(P1.x - P2.x)$ and $F_{a_y} = k_a \times \text{abs}(P1.y - P2.y)$, where k_a is the attractive factor. If one of the pins is an IO port, k_a is equal to the attractive factor multiplied by the IO factor (default = 1.0).

Repulsive force (F_r) applies only to nodes that overlap with each other. We indicate the center coordinates of each node M using $(M.x, M.y)$. For two nodes $M1$ and $M2$ that overlap with each other, the repulsive force components applied to $M1$ and $M2$ are $F_{r_x} = k_r \times F_{r_{max}} \times \frac{\text{abs}(M1.x - M2.x)}{\text{dist}(M1, M2)}$ and $F_{r_y} = k_r \times F_{r_{max}} \times \frac{\text{abs}(M1.y - M2.y)}{\text{dist}(M1, M2)}$, where k_r is the repulsive factor, $F_{r_{max}}$ is the maximum move distance (see Eq. 1) and $\text{dist}(M1, M2)$ is the Euclidean distance between the centers of $M1$ and $M2$.

The net force exerted on the i^{th} standard-cell cluster is calculated and then normalized according to

$$F_i = F_{i_a} + F_{i_r}$$

$$\max_move_distance = \frac{\max(width,height)}{num_iters}$$

$$F_{i_x} = \frac{F_{i_x}}{\max_j(\{|F_{j_x}\})} \times \max_move_distance \quad (1)$$

$$F_{i_y} = \frac{F_{i_y}}{\max_j(\{|F_{j_y}\})} \times \max_move_distance$$

where *width* and *height* are respectively the width and height of the canvas, *num_iters* is the number of iterations, and $\max_j(\{|F_{j_x}\})$ and $\max_j(\{|F_{j_y}\})$ are respectively the maximum absolute values of horizontal and vertical forces over all nodes. Finally, the standard-cell clusters are moved based on the normalized forces exerted on them. Any move that will push a standard-cell cluster outside of the canvas is canceled. Our open-source implementation of FD is available in *MacroPlacement* [39]. [39] gives a comparison of results from our FD and *CT*'s FD for the Ariane testcase.

3.2.2 Proxy cost calculation. The **proxy cost** R is the weighted sum of wirelength, density and congestion cost, i.e.,

$$R = Wirelength + \gamma \times Density + \lambda \times Congestion \quad (2)$$

where λ and γ are both equal to 0.5 by default. Proxy cost is crucial to understand, since it drives the RL agent's learning and comprises the only apparent connection between *CT* and optimization of "key metrics, including power consumption, performance and chip area" (see also Table 1 in *Nature*). We now describe the three components of proxy cost, with an emphasis on congestion cost. First, the *Wirelength* cost is the normalized half-perimeter wirelength (HPWL), defined as

$$Wirelength = \frac{1}{|nets|} \sum_{net} \frac{net.weight \times HPWL(net)}{width + height}$$

where *width* and *height* are respectively the width and height of the canvas. Second, the *Density* cost is the average density of the top 10% densest grid cells. Third, *Congestion* cost is decomposed into two parts: congestion due to macros (*macro_cong*) and congestion due to net routing (*net_cong*). In the example of Figure 1, the horizontal congestion of grid cell g_1 ($H_cong_{g_1}$) is the sum of the macro congestion ($H_macro_cong_{g_1}$) induced by macro M1 (the large green rectangle) and the routing congestion ($H_net_cong_{g_1}$) induced by the routing pattern of net N1 (the orange path).

Computation of macro congestion. Macro congestion is induced by the extra routing layer resources used by macros. When calculating macro congestion, the horizontal and vertical *macro_cong* values of a grid cell g are, respectively, the summation of the routing resources used by macros that intersect g 's right and top boundaries. Full details are provided in [50] [35].

Computation of routing congestion. Routing congestion is induced by the routing resources occupied by each routed net. In *CT*'s proxy cost calculation, a net is routed based on the number of different grid cells occupied by its pins. (All pins of a given net that are within a single grid cell are considered as a single pin when computing routing congestion.) A k -grid net is a net whose pins occupy k different grid cells. The grid cell occupied by a net's source pin is the *source grid cell* of the net, and other grid cells occupied by the net's pins are *sink grid cells*. Then, the routing pattern of a k -grid net is calculated as follows. (i) A 1 -grid net is ignored. (ii) A 2 -grid net is routed using an "L" that depends on

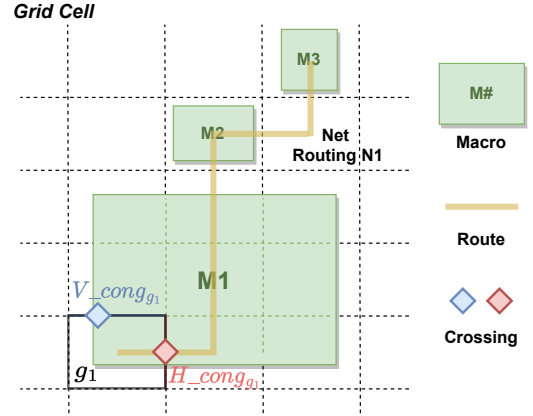


Figure 1: Illustration for congestion cost computation.

relative locations of the source and sink grid cells. (iii) A 3 -grid net has routing pattern determined by relative positions of its three different grid cells. (iv) A k -grid net, $k > 3$, is decomposed into $k - 1$ 2 -grid nets using a star model centered at the source pin (grid cell). The routing congestion contributions from all nets are superposed. Then, smoothing of H_net_cong and V_net_cong values per grid is performed. Full details are provided in [35].

Computation of congestion cost. After computing macro congestion and routing congestion, the total congestion for each grid cell is obtained by adding macro congestion and routing congestion for each direction separately, i.e.,

$$H_cong = H_macro_cong + H_net_cong$$

$$V_cong = V_macro_cong + V_net_cong$$

Then, congestion cost is given by the average of the top 5% of all H_cong and V_cong values of grid cells in the canvas. Our open-source implementation of proxy cost calculation is available in the *MacroPlacement* repository [35]. [47] gives a comparison of our and *CT*'s calculations for the Ariane testcase.

3.3 Simulated Annealing

Simulated Annealing (SA) is used as a baseline for comparison by both *Nature* and *SB*. We implement and run SA based on the description given in the *SB* manuscript; Table 2 of [11] gives a concise comparison of hyperparameters used by *SB* and *Nature*. Our implementation differs from that described in *Nature* in its use of *move* and *shuffle* in addition to *swap*, *shift* and *mirror* actions. We also use two initial macro placement schemes, i.e., "spiral macro placement" whereby macros are sequentially placed around the boundary of the chip canvas in a counterclockwise spiral manner, and "greedy packer" whereby macros are packed in sequence from the lower-left corner to the top-right corner of the chip canvas [11]. FD placement (Sec. 3.2.1) is used to update the locations of standard-cell clusters every $\{2n, 3n, 4n, 5n\}$ macro actions, where n is the number of hard macros; FD is not itself an action. The SA cost function is the proxy cost described in Sec. 3.2.2. Our SA implementations are open-sourced in *MacroPlacement* [36]; the C++ implementations of FD and proxy cost calculation are used in our reported SA experiments.

4 MODERN BENCHMARKS AND COMMERCIAL EVALUATION FLOW

We now describe testcases and design enablements that have been developed to improve academic research foundations while also serving the *MacroPlacement* effort. In addition, we present the commercial evaluation flow that we use to assess various macro placement solutions.

4.1 Testcases and enablements

New, macro-heavy testcases and enhanced design enablements have been developed and made available in *MacroPlacement*.

Testcases. *MacroPlacement* includes four open-source testcases: Ariane [13] (20K FFs, 133 and 136 macros), BlackParrot (Quad-Core) [14] (214K FFs, 220 macros), MemPool Group [15] (361K FFs, 324 macros), and NVDLA (partition “c”) [25] (45K FFs, 128 macros). All macros in Ariane and in NVDLA have the same size, while BlackParrot and MemPool Group each contain macros of varying sizes. Our experiments use the 133-macro Ariane variant to match the Ariane in *Nature* and *CT*. [40] gives details of testcase creation.

Enablements. *MacroPlacement* includes three open-source enablements: SKY130HD [19], NanGate45 [16] and ASAP7 [18]. We use the *bsg_fakeram* [17] generator to generate SRAMs for SKY130HD and NanGate45 enablements. The SKY130HD PDK has only five metal layers, while SRAMs typically use or block the first four metal layers; this makes it difficult to route macro-heavy testcases. We therefore provide the SKY130HD FakeStack [41] enablement which contains nine metal layers. We also provide FakeRAM2.0 [20] to generate SRAM abstracts for ASAP7-based testcases.

4.2 Commercial evaluation flow

Figure 2 presents the commercial tool-based flow that we use to create macro placement instances and evaluate macro placement solutions.¹ The flow has the following steps.

Step 1: We run logic synthesis using Cadence Genus 21.1 to synthesize a gate-level netlist for a given testcase.

Step 2: We input the synthesized netlist to Cadence Innovus 21.1 and use CMP (Concurrent Macro Placer) to place macros.

Step 3: We input the floorplan .def with placed macros to the Cadence Genus iSpatial flow and run physical-aware synthesis. The physical-aware synthesis is used to generate initial placement locations (i.e., (x,y) coordinates) for all standard cells.

Step 4: We obtain macro placement solutions from six methods: *CT*, *SA*, *RePlace*, *AutoDMP*, *CMP* and human-expert. (The *CMP* macro placement is produced in Step 2.) Before running *CT* or *SA* macro placement, we convert the verilog netlist to protocol buffer (protobuf) format, and use *CT-Grouping* to generate standard-cell clusters. The initial placement of standard cells obtained in Step 3 is used to guide the *CT-Grouping* process. Code to generate the protobuf netlist and group standard cells are available in *MacroPlacement*.² To generate a Bookshelf-format input netlist for *RePlace*, we use the LEF/DEF to Bookshelf converter from RosettaStone [4]. *RePlace*, *AutoDMP* and human experts are not given any initial placement information for standard cells or macros.

¹We do not perform any benchmarking of the EDA tools used in this study.

²For the *CT* and *SA* runs reported here, we run the grouping flow provided in Google’s *CT* after generating the protobuf netlist.

Step 5: For each macro placement solution, we input the floorplan .def with macro placement locations to Innovus for place and route (P&R). After reading the .def file into Innovus, we set all standard cells to unplaced, and legalize macro locations using the `refine_macro_placement` command.³ We then perform power delivery network (PDN) generation.⁴ After PDN generation, we run placement, clock tree synthesis, routing and post-route optimization (postRouteOpt).

Step 6: We extract the total routed wirelength (rWL), standard cell area, total power, worst negative slack (WNS), total negative slack (TNS) and DRC count from the post-routed design. Table 1 of the *Nature* paper [9] presents similar metrics to compare different macro placement solutions.⁵ Below, we refer to these metrics as the (*Nature*) “Table 1 metrics”.

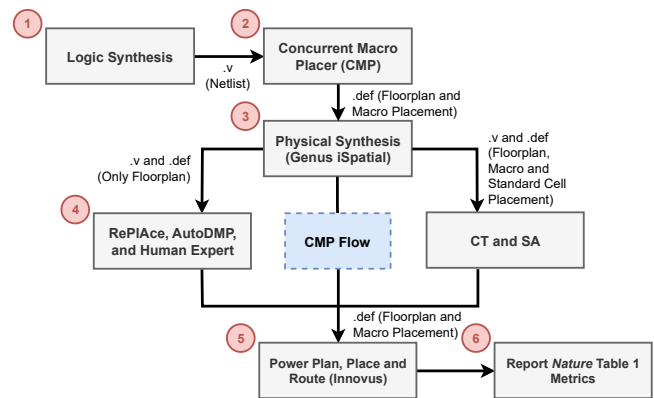


Figure 2: Evaluation flow for macro placement solutions produced by different macro placers.

5 EXPERIMENTS AND RESULTS

In this section, we first study the performance of *CT* and other macro placers. We then present experimental results for ablation, stability, and other studies. The results that we present are a subset of what is summarized in [34] and [37].

5.1 Comparison of *CT* with other macro placers

Configuration of different macro placers. We generate macro placement solutions using *CT*, *CMP*, *SA*, *RePlace* and *AutoDMP*. We also include macro placement solutions generated by human-experts. For *CT* runs, we follow the default setting given in [23], except that we use density weight 0.5 instead of 1.0, based on guidance from Google engineers [27]. For *CMP*, we use the default tool settings. For *SA*, we use the configurations described in [11] and the C++ implementation available in *MacroPlacement*. Instead of

³Macro placements produced by *RePlace*, *AutoDMP*, *CT* and *SA* can have macros that are not placed on grids.

⁴*CT* assumes that 18% of routing tracks are used by PDN [45]. We implement our PDN scripts following the “18% rule” for all the enablements. All of our PDN scripts are available at [46] in *MacroPlacement*.

⁵According to *Nature* authors, “The final metrics in Table 1 are reported after PlaceOpt, meaning that global routing has been performed by the EDA tool”. In this paper, we report metrics after postRouteOpt, meaning that the entire P&R flow has been performed. A number of results reported in [34] include metrics after both PlaceOpt and postRouteOpt.

four random seeds, we use two random seeds {0, 1} and two initialization methods [*greedy packing*, *spiral initialization*]. We run in parallel 320 SA workers for 12.5 hours and use the macro placement solution with minimum proxy cost as the final SA solution. The SA workers do not communicate with each other. RePlace is run with the default parameters given in [22] except that we change *pcofmax* to 1.03 from the default value of 1.05. We run AutoDMP [1] for 200 samples with two GPU workers, default configuration space, and *ppa_cost* score function. In all experiments, we use Genus 21.1 for synthesis (Step 1) and Innovus 21.1 for place and route (Steps 5 and 6).

Evaluation of Table 1 metrics for different macro placers. We generate macro placement solutions using testcases in open NanGate45 (NG45) and commercial GlobalFoundries 12nm (GF12) enablements. Table 1 presents *Nature Table 1* metrics obtained using the evaluation flow of Figure 2 for different macro placers on our testcases. The *Table 1* metrics in GF12 are normalized to protect foundry IP: (i) standard-cell area is normalized to core area; (ii) total power and rWL are normalized to the *CT* result; and (iii) timing metrics (WNS, TNS) are normalized to the target clock period (TCP) which we leave unspecified.⁶ In NG45, the respective default TCP values for Ariane, BlackParrot Quad-Core (BlackParrot) and MemPool Group (MemPool) are 1.3ns, 1.3ns and 4.0ns. All testcases reported in Table 1 have 68% floorplan utilization, matching the Ariane design that is public in *CT*. Studies of other testcases and enablements are pending (updates will be posted in [34]).

Table 1 also reports the *CT* proxy cost for all macro placement solutions, as evaluated by the *plc_client* provided in *CT*. To compute the proxy cost for CMP, RePlace, AutoDMP and human-expert solutions, we first update hard macro locations and orientations, then run the FD placer to place all standard-cell clusters (soft macros). We then compute the proxy cost. Figure 3 shows Ariane-NG45 macro placements produced by the macro placers we study.⁷ We make the following observations.

- **Comparison of routed wirelength (rWL):** CMP and AutoDMP consistently dominate the other macro placers (we comment on this in Footnote 11 below). For BlackParrot-GF12, AutoDMP’s rWL is ~40% less than that of *CT*.
- **Comparison of proxy cost:** SA dominates other macro placers in 4 out of 6 cases, and *CT* dominates other macro placers in 2 out of 6 cases.
- **Comparison between *CT* and Human experts:** For large macro-heavy designs such as BlackParrot and MemPool, human experts outperform *CT* in terms of the *Nature Table 1* metrics of “ground truth” postRouteOpt outcomes.
- **Comparison between *CT* and SA:** *CT* generates better TNS than SA for 4 of 6 cases, while SA generates better rWL (5 of 6 cases) and proxy cost (4 of 6 cases) than *CT*.
- **Insertion of *CT* into a standard EDA flow:** The commercial evaluation flow for *CT* is equivalent to the CMP flow with insertion of the *CT* macro placement step. *CT* outcomes have better proxy cost but worse rWL than the “pure EDA flow”.

⁶The WNS and TNS timing metrics reported in Table 1 suggest that the TCP for BlackParrot-GF12 should be reduced, while the TCP for MemPool-GF12 should be increased. Ongoing studies adjust TCPs for these designs and will be reported in [34].

⁷All postRouteOpt designs are DRC-clean, with the exception of *CT*, SA and AutoDMP outcomes for MemPool-NG45; these respectively have 5K, 45K and 31K DRC violations. We are unable to successfully run RePlace for the MemPool testcase.

Table 1: *Nature Table 1* metrics of different macro placers for testcases in open NG45 and commercial GF12 enablements. Data points for GF12 (excluding proxy cost) are normalized. We highlight best values of metrics in blue bold font.

Design Enablement	Macro Placer	Area (μm^2)	rWL (mm)	Power (mW)	WNS (ps)	TNS (ns)	Proxy Cost
Ariane NG45	CT	244,022	4,894	828.7	-79	-25.8	0.857
	CMP	256,230	4,057	851.5	-154	-196.5	1.269
	RePlace	252,444	4,609	843.9	-103	-69.9	1.453
	SA	248,344	4,014	831.9	-111	-87.0	0.752
	AutoDMP	243,720	3,764	821.7	-95	-37.5	1.247
	Human	249,034	4,681	832.4	-88	-46.8	1.158
BlackParrot NG45	CT	1,956,712	36,845	4627.4	-185	-1040.8	1.021
	CMP	1,916,166	23,144	4428.7	-144	-356.2	1.022
	RePlace	1,957,915	32,970	4591.5	-252	-6723.2	1.346
	SA	1,935,896	30,927	4523.7	-156	-1839.8	0.921
	AutoDMP	1,920,024	23,376	4438.6	-190	-1183.1	1.007
	Human	1,919,928	25,916	4469.6	-97	-321.9	1.275
MemPool NG45	CT	4,890,644	123,330	2760.5	-69	-119.3	1.253
	CMP	4,837,150	102,907	2586.6	-20	-1.0	1.571
	SA	4,948,800	125,682	2805.8	-124	-11.7	1.489
	AutoDMP	4,884,674	110,982	2658.8	-115	-43.4	1.782
	Human	4,873,872	107,598	2640.0	-49	-11.9	1.733
	Note: Data points (excluding proxy cost) for GF12 are normalized.						
Ariane GF12	CT	0.138	1.000	1.000	-0.145	-123.4	0.706
	CMP	0.139	0.865	0.990	-0.159	-142.3	0.878
	RePlace	0.140	1.042	1.015	-0.168	-197.4	1.160
	SA	0.139	0.925	0.995	-0.155	-178.0	0.664
	AutoDMP	0.137	0.885	0.985	-0.130	-90.5	0.972
	Human	0.137	1.064	0.981	-0.139	-106.6	1.125
BlackParrot GF12	CT	0.179	1.000	1.000	0.001	0.000	0.789
	CMP	0.178	0.593	0.918	0.001	0.000	0.844
	RePlace	0.178	0.798	0.959	0.000	0.000	1.121
	SA	0.178	0.731	0.944	0.000	0.000	0.665
	AutoDMP	0.178	0.587	0.917	0.000	0.000	0.816
	Human	0.178	0.642	0.928	0.000	0.000	1.089
MemPool GF12	CT	0.410	1.000	1.000	-0.195	-1849.4	0.984
	CMP	0.405	0.821	0.895	-0.197	-1961.3	1.422
	SA	0.412	0.991	1.000	-0.187	-2442.7	1.196
	AutoDMP	0.402	0.843	0.895	-0.213	-1015.7	1.448
	Human	0.406	0.888	0.920	-0.149	-1766.5	1.446

5.2 Ablation, Stability and Other Studies

We now give a sampling of results and takeaways from various ablation, stability and other studies.

5.2.1 *CT* is helped by placement from physical synthesis. As noted in Sec. 3.1, *CT* relies on placement locations in its input, though this is not mentioned in *Nature*. To test the effect of initial placement on the *CT* outcome, we generate three “vacuous” input placements for the Ariane-NG45 design. Cases (1), (2) and (3) respectively have all standard cells and macros located at (600, 600), at the lower-left corner (0, 0), and at the upper-right corner (1347.1, 1346.8). For each case, we generate the clustered netlist, run *CT* and collect *Table 1* metrics, following the evaluation flow of Sec. 4.2. We find that placement information in the input provides significant benefit to *CT*: given locations from Cadence CMP and Genus iSpatial (Steps 2 and 3 of Figure 2), *CT*’s solution has rWL that is 10.32%, 7.24% and 8.17% less than in Cases (1), (2) and (3), respectively. The *Table 1* metrics of all three runs are given at [38] in *MacroPlacement*.

5.2.2 Both physical synthesis tools lead to similar *CT* outcomes. The evaluation flow in Figure 2 uses Cadence CMP and Genus iSpatial. We have also used Synopsys Design Compiler Topographical version R-2020.9 to run physical-aware synthesis and generate

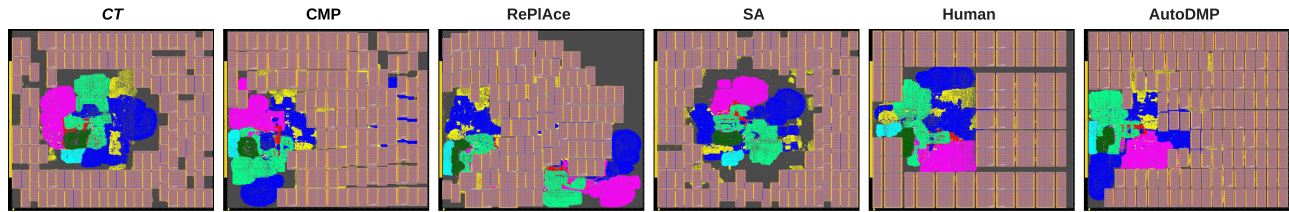


Figure 3: Ariane-NG45 (68% utilization, 1.3ns TCP) macro placements generated by different macro placers.

standard-cell and macro placement locations, for the Ariane-NG45 design. We observe similar outcomes with either physical synthesis tool; details of *Nature Table 1* metrics are given at [48].

5.2.3 Proxy cost is not well-correlated to Nature Table 1 metrics. Since the RL agent in *Nature* and *CT* is driven by proxy cost, we examine the correlation of proxy cost with *Nature Table 1* metrics. We collect 15 macro placement solutions generated by *CT* for Ariane-NG45 that have proxy cost less than 0.9, and generate the *Table 1* metrics for each macro placement (details are given at [44]). Table 2 shows the Kendall rank correlation coefficient for proxy cost and *Table 1* metrics. Values close to +1 or -1 indicate strong correlation or anticorrelation, respectively, while values close to 0 indicate a lack of correlation. Thus, in the regime of relatively low proxy cost, we observe poor correlation of proxy cost and its components with *Table 1* metrics.

Table 2: Kendall rank correlation coefficient between proxy cost and *Nature Table 1* metrics.

Proxy Cost Element	Std Cell Area	rWL	Power	WNS	TNS
Wirelength	-0.221	0.317	-0.144	0.163	0.317
Congestion	-0.029	0.086	-0.010	0.105	-0.048
Density	0.096	0.230	0.096	0.268	0.077
Proxy	-0.010	0.257	0.048	0.200	0.048

5.2.4 SA gives more stable results than CT. *CT* results can vary even if the same global seed is used, due to stochasticity in training. *SA* results are deterministic for any given seed, but vary across different seeds. We empirically assess the stability of *CT* and *SA* results across different seeds, by recording the mean and standard deviation of the overall proxy cost, proxy cost components, and *Nature Table 1* metrics. Table 3 gives results for *CT*, where six runs are made for each of three seeds, i.e., a total of 18 training runs. Table 4 gives results for *SA*, where six runs are made with different seeds. Note that a single run of *SA* is configured with a pair of seeds; half of the run’s 320 independent threads use the first seed, and the other half use the second seed. From (aggregated) proxy cost metrics and *Nature Table 1* metrics, we observe that *SA* exhibits significantly smaller standard deviation than *CT*. Timing metrics (WNS, TNS) show larger variation than other *Table 1* metrics.

5.2.5 Confirmation of CT setup and execution. As noted above, Google engineers have generously provided clarifications and guidance over the course of our efforts. An early confirmation of our *CT* setup and execution methodology involved Google engineers running *CT* in-house on the clustered netlist of Ariane in NG45 with

Table 3: Mean (standard deviation) of proxy cost and *Nature Table 1* metrics for different global seeds in *CT*.

Metric	CT Cost Metrics				Nature Table 1 Metrics				
	Proxy Cost	WL Cost	Den. Cost	Cong. Cost	Area (μm^2)	Power (mW)	rWL (mm)	WNS (ps)	TNS (ns)
Ariane-NG45									
111	0.841 (0.012)	0.105 (0.002)	0.525 (0.013)	0.949 (0.014)	246,651 (1,258)	834.2 (2.4)	4,880 (137)	-102 (27)	-68.3 (40.5)
222	0.924 (0.035)	0.106 (0.006)	0.529 (0.024)	1.107 (0.050)	247,755 (1,776)	836.5 (5.7)	5,114 (433)	-112 (37)	-79.5 (39.7)
333	0.914 (0.033)	0.106 (0.003)	0.529 (0.012)	1.086 (0.057)	246,855 (1,926)	833.7 (3.9)	4,941 (97)	-87 (20)	-48.0 (28.3)
AGGR	0.893 (0.046)	0.106 (0.003)	0.528 (0.016)	1.047 (0.08)	247,087 (1,652)	834.8 (4.1)	4,978 (272)	-100 (28)	-65.3 (36.9)
BlackParrot-NG45									
111	1.059 (0.064)	0.074 (0.009)	0.802 (0.051)	1.169 (0.061)	1,957,636 (10,955)	4,646.3 (76.2)	37,699 (4,382)	-200 (39)	-1342.5 (1171.5)
222	1.064 (0.040)	0.072 (0.004)	0.820 (0.022)	1.163 (0.053)	1,957,891 (8,215)	4,628.9 (38.2)	36,849 (1,888)	-221 (41)	-1707.6 (974.2)
333	1.097 (0.043)	0.077 (0.005)	0.851 (0.048)	1.189 (0.032)	1,959,685 (6,004)	4,656.0 (34.8)	39,159 (2,348)	-189 (36)	-986.8 (458.4)
AGGR	1.073 (0.050)	0.074 (0.006)	0.824 (0.045)	1.173 (0.048)	1,958,404 (8,162)	4,643.7 (51.3)	37,902 (3,046)	-203 (39)	-1345.6 (914.5)

Table 4: Mean (standard deviation) of proxy cost and *Nature Table 1* metrics for different global seeds in *SA*.

Metric	CT Cost Metrics				Nature Table 1 Metrics				
	Proxy Cost	WL Cost	Den. Cost	Cong. Cost	Area (μm^2)	Power (mW)	rWL (mm)	WNS (ps)	TNS (ns)
Ariane-NG45									
0, 1	0.752	0.085	0.499	0.835	248,343	831.9	4,014	-111	-87.0
2, 3	0.751	0.085	0.498	0.834	244,218	827.2	4,023	-103	-72.2
4, 5	0.755	0.087	0.497	0.839	245,604	830.7	4,062	-197	-229.7
6, 7	0.754	0.088	0.500	0.833	247,213	831.6	4,128	-141	-117.0
8, 9	0.752	0.085	0.501	0.833	246,159	828.8	3,992	-111	-56.4
10, 11	0.755	0.086	0.5007	0.8378	247,820	832.4	3,990	-135	-133.9
AGGR	0.753 (0.002)	0.086 (0.001)	0.499 (0.002)	0.835 (0.002)	246,560 (1,533)	830.4 (2.0)	4,035 (53)	-133 (35)	-116.0 (62.5)
BlackParrot-NG45									
0, 1	0.921	0.064	0.708	1.06	1,935,896	4,523.7	30,927	-156	-1839.8
2, 3	0.921	0.062	0.720	0.999	1,939,640	4,529.8	30,499	-219	-1857.3
4, 5	0.926	0.059	0.732	1.001	1,937,104	4,516.3	29,696	-216	-1880.5
6, 7	0.921	0.062	0.735	0.983	1,936,302	4,526.0	31,010	-181	-733.0
8, 9	0.923	0.058	0.729	1.001	1,934,343	4,514.3	29,495	-183	-472.5
10, 11	0.931	0.063	0.748	0.988	1,936,369	4,533.5	31,121	-172	-718.6
AGGR	0.924 (0.004)	0.061 (0.002)	0.729 (0.014)	0.996 (0.009)	1,936,609 (1,745)	4,523.9 (7.5)	30,458 (703)	-188 (25)	-1250.3 (673.6)

68% utilization and 4ns TCP. Figure 4 shows the *CT* training curves generated by us and by Google engineers. Running the evaluation flow on both macro placement solutions produces similar *Nature Table 1* metrics, as detailed in [49].

5.2.6 Ariane is less challenging than other testcases. We perform a *shuffling* experiment to evaluate the relative difficulty of finding

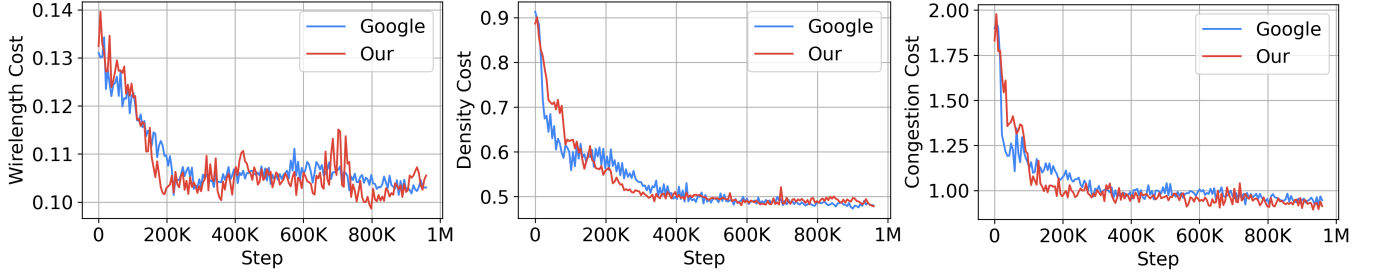


Figure 4: CT training curves of Ariane in NG45, generated by us and by Google engineers.

good solutions for different testcases. Starting from the *CT* macro placement, we randomly shuffle the locations of same-size macros and generate six macro placements corresponding to six different random seeds. During macro shuffling, when macro A moves to the initial location of macro B, we update the orientation of macro A with the initial orientation of macro B. We then run the evaluation flow and generate *Table 1* metrics for each macro placement.

Table 5 shows the average change in *Table 1* metrics and P&R runtime (Steps 5 and 6 of Figure 2) for shuffled macro placements, relative to the original *CT* macro placement. For Ariane, shuffling increases rWL by 16.17% and P&R runtime by 8.17%. For BlackParrot, shuffling increases rWL by 33.51% and P&R runtime by 23.76%. Because Ariane has less degradation of *Table 1* metrics with shuffling, we consider Ariane to be a less difficult testcase than BlackParrot. Details of *Table 1* metrics for all the macro placements generated using macro shuffling are available at [43]. Macro shuffling for MemPool resulted in flow failure for all runs, suggesting that MemPool is even more difficult than BlackParrot.

Table 5: Average change of *Table 1* metrics and P&R runtime due to macro shuffling (Ariane, BlackParrot).

Design	Standard Cell Area	rWL	Total Power	Runtime
Ariane	1.75%	16.17%	1.49%	8.17%
BlackParrot	2.23%	33.51%	6.54%	23.76%

6 ACADEMIC BENCHMARKS AND EVALUATION FLOW

The *SB* manuscript [11] opened the question of assessment using standard benchmarks from the VLSI CAD physical design field. We assess *CT* on the ICCAD04 Mixed-size Placement benchmarks [21] studied in *SB*. 17 testcases contain macros, with number of macros ranging from 178 to 786 and number of standard cells ranging from 12K to 210K; each testcase has multiple macro sizes. Here, we describe our academic evaluation flow and then compare the performance of *CT*, *SA* and *RePlace*. We also study the effect of proxy cost weighting on the *CT* vs. *SA* comparison.

Academic evaluation flow. Figure 5 shows the academic tool-based flow used to create macro placement instances and evaluate macro placement solutions. Our six-step flow enables comparison according to both HPWL and proxy cost, as in *SB*. (1) We take the netlist in Bookshelf format as input, and run *RePlace* [22] and *NTUplace3* [26] to generate initial placement locations (i.e., (x,y) coordinates) for all standard cells and macros. HPWL for *RePlace*

is reported at this point.⁸ (2) We convert the placed netlist (Bookshelf format) into *CT*'s protobuf format. (3) We use *CT*-Grouping to generate standard-cell clusters, with macro spacing = 0.0 (default = 0.1) and cell_area_utilization = 1.0 (default = 0.5) to handle high area utilizations. (4) We run *FD* with only repulsive forces (attractive factor $k_a = 0$) on the clustered netlist to reduce overlap between standard-cell clusters. Proxy cost for *RePlace* is reported at this point. (5) We run *CT* and *SA* to minimize proxy cost on the clustered netlist. Proxy cost for *CT* and *SA* is reported at this point. (6) After running *CT* or *SA*, we fix the locations of macros and run *RePlace* and *NTUplace3* to place standard cells. HPWL for *CT* or *SA* is reported at this point. Settings for *CT*, *SA* and *RePlace* are as described in Sec. 5.1, and all runscripts are provided at [50].

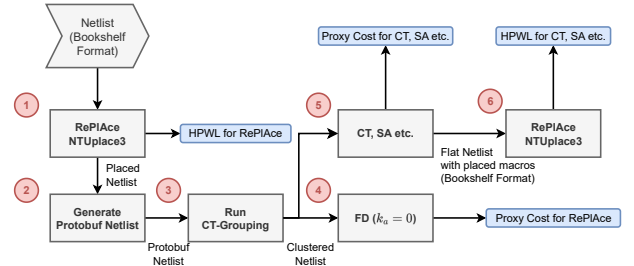


Figure 5: Academic evaluation flow for macro placers.

Comparison of *CT* with *SA* and *RePlace*. Table 6 presents results for *CT*, *SA* and *RePlace* on ICCAD04 testcases. We observe the following. (i) In terms of proxy cost, *RePlace* is always better than *SA*, and *SA* is always better than *CT*.⁹ (ii) In terms of HPWL, *RePlace* is better than *SA* for 15 of 17 testcases, and *SA* is better than *CT* in 16 of 17 testcases. (iii) Our *RePlace* runs obtain similar HPWL to that reported in *SB*'s Table 1. (iv) Compared to *SB*'s Table B2, our *SA* runs produce better HPWL than *SB*'s *SA* in 10 out of 17 testcases, and our *CT* runs produce worse HPWL than *SB*'s *CT* in 15 out of 17 testcases.¹⁰

⁸LEF/DEF versions of these testcases are malformed; hence, only Bookshelf versions can be used, and commercial EDA tools cannot be run.

⁹*RePlace* is superior to *CT* in every element of proxy cost, across all ICCAD04 testcases. However, this would not necessarily translate to production contexts where *Nature Table 1* metrics such as congestion would apply. Indeed, as integrated into the OpenROAD open-source P&R tool [2], *RePlace* has undergone significant changes for improved routability and timing-driven quality of results [32].

¹⁰Our proxy cost values cannot be compared with those in the *SB* manuscript, since routing resource assumptions used to compute congestion cost in *SB* are unknown. Density and congestion weights required to compute proxy cost are also unknown.

Table 6: Proxy cost and HPWL of CT, SA and RePLace for ICCAD04 testcases.

Design	CT		SA		RePLace	
	Proxy Cost	HPWL	Proxy Cost	HPWL	Proxy Cost	HPWL
ibm01	1.6617	3,373,670	1.3166	2,546,110	0.9976	2,241,590
ibm02	2.2130	6,281,060	1.9072	5,118,090	1.8370	5,265,410
ibm03	2.0316	9,353,340	1.7401	7,456,430	1.3222	6,344,390
ibm04	1.7542	9,781,980	1.5037	8,445,470	1.3024	7,112,910
ibm06	2.9395	7,097,540	2.5057	6,334,540	1.6187	5,725,280
ibm07	2.2191	13,060,600	2.0229	11,956,000	1.4633	9,813,440
ibm08	2.3428	15,684,500	1.9239	14,093,200	1.4285	11,185,400
ibm09	1.6998	15,691,200	1.3875	13,222,300	1.1194	11,940,500
ibm10	2.5972	54,718,400	2.1108	37,128,500	1.5009	39,453,000
ibm11	1.8916	21,647,400	1.7111	20,723,300	1.1774	16,589,100
ibm12	3.1022	48,175,200	2.8261	40,259,300	1.7261	30,497,500
ibm13	1.9785	29,679,600	1.9141	27,099,500	1.3355	21,832,200
ibm14	2.4594	51,257,200	2.2750	43,863,600	1.5436	33,917,600
ibm15	2.7759	54,563,400	2.3000	50,491,900	1.5159	44,368,200
ibm16	2.3018	68,664,000	2.2337	65,699,600	1.4780	51,509,800
ibm17	4.0724	81,895,000	3.6726	76,482,600	1.6446	62,749,100
ibm18	3.2188	43,119,400	2.7755	43,784,200	1.7722	39,705,400

Table 7: CT and SA results for ibm09 and ibm15 using different weight combinations in proxy cost (Eq. 2).

Design (CT/SA)	(γ, λ)	WL Cost	Den. Cost	Cong. Cost	Proxy Cost	HPWL
ibm09 (CT)	(0.5, 0.5)	0.098	0.873	2.331	1.700	15,691,200
	(1, 0.5)	0.100	0.818	2.407	2.122	15,508,600
	(0.01, 0.01)	0.095	0.904	2.679	0.1304	15,129,200
ibm09 (SA)	(0.5, 0.5)	0.091	0.749	1.845	1.387	13,222,300
	(1, 0.5)	0.100	0.737	1.981	1.828	14,119,400
	(0.01, 0.01)	0.079	0.934	2.233	0.111	14,713,400
ibm15 (CT)	(0.5, 0.5)	0.103	1.022	4.323	2.776	54,563,400
	(1, 0.5)	0.101	0.932	3.572	2.819	52,283,200
	(0.01, 0.01)	0.093	1.049	4.229	0.146	53,496,800
ibm15 (SA)	(0.5, 0.5)	0.093	0.971	3.443	2.300	50,491,900
	(1, 0.5)	0.094	0.977	3.448	2.795	50,235,500
	(0.01, 0.01)	0.086	1.146	3.927	0.136	51,834,900

CT vs. SA is stable across proxy cost weighting. For a multi-objective optimization (wirelength, density and congestion), reward engineering is very important in practice. Following a suggestion from [31], we explore alternative proxy cost weighting to potentially improve final CT outcomes for ICCAD04 testcases. We study three weight combinations (see Sec. 3.2.2): (1) $\gamma = 0.5, \lambda = 0.5$ (suggested by Google Brain [27]); (2) $\gamma = 1.0, \lambda = 0.5$ (default setting of CT); and (3) $\gamma = 0.01, \lambda = 0.01$ (default setting of Nature). Table 7 shows that SA consistently achieves lower proxy cost than CT for ibm09 and ibm15 across the different weight combinations.

7 CONCLUSION

Google’s Nature paper [9] and the subsequent release of Circuit Training in GitHub [23] have drawn broad attention throughout the EDA and IC design communities. The work presents a novel orchestration of multiple elements: (i) a proxy cost function that captures wirelength, density and congestion and is efficiently evaluated with FD placement; (ii) a sequential framework for macro placement; (iii) gridding of the layout canvas whereby macros can be placed

on centers of grid cells, thus reducing the solution space for macro locations; and (iv) clustering of standard cells based on an initial physical-synthesis placement, which reduces both the size of the graph input to GNN and the runtime of proxy cost evaluation. The “News and Views” commentary [5] that accompanied the Nature paper noted, “We can therefore expect the semiconductor industry to redouble its interest in replicating the authors’ work” – and this is indeed what has transpired since June 2021.

To date, the bulk of data used by Nature authors has not been released, and key portions of source code remain hidden behind APIs. This has motivated our efforts toward open, transparent implementation and assessment of Nature and CT. MacroPlacement provides open testcases, design enablements, commercial and academic evaluation flows, and experimental evaluations to clarify inconsistencies and gaps seen in Nature and CT. Throughout our work, Google engineers have provided guidance and clarifications.

Our experiments show the following. (i) Poor quality of initial placement in the CT input can degrade rWL by up to 10%. The use of initial placement locations from physical synthesis is an important element of CT. (ii) SA produces better proxy cost than CT for modern testcases (4/6) and ICCAD04 testcases (17/17), as well as across varying weight combinations that we study. (iii) For large macro-heavy designs such as BlackParrot and MemPool, human experts outperform CT in terms of Nature Table 1 metrics. This being said, developing a proxy cost with higher correlation to Nature Table 1 metrics will likely improve the “ground truth” performance of CT. (iv) Analytical macro placers (e.g., DREAMPlace in AutoDMP) produce better routed wirelength compared to CT and SA. Replacing the force-directed placement used in Nature with analytical mixed-size placement is likely to improve wirelength.¹¹

The difficulty of reproducing methods and results of [9], and the effort spent on MacroPlacement, highlight potential benefits of a “papers with code” culture change in the academic EDA field. Recent policy changes of EDA vendors are a laudable step forward; they enable us to include Tcl scripts for commercial SP&R flows in the MacroPlacement GitHub. Contributions of benchmarks, design enablements, implementation flows and additional studies to the MacroPlacement effort are warmly welcomed.

ACKNOWLEDGMENTS

We thank David Junkin, Patrick Haspel, Angela Hwang and their colleagues at Cadence and Synopsys for policy changes that permit our methods and results to be reproducible and sharable in the open, toward advancement of research in the field. We thank many Google engineers (Azalia Mirhoseini, Anna Goldie, Mustafa Yazgan, Eric Johnson, Roger Carpenter, Sergio Guadarrama, Guanhang Wu, Joe Jiang, Ebrahim Songhori, Young-Joon Lee and Ed Chi) for their time and discussions to clarify aspects of Circuit Training, and to run their internal flow with our data. We thank Ravi Varadarajan for early discussions and flow setup, and Mingyu Woo for guidance on RePLace versions and setup. Support from NSF CCF-2112665 (TILOS) and DARPA HR0011-18-2-0032 (OpenROAD) is gratefully acknowledged.

¹¹The latest release of CT [24] replaces force-directed placement with DREAMPlace [6]. We understand that for a given fixed macro placement, DREAMPlace not only reduces HPWL of the clustered standard-cell placement compared to FD, but has better correlation to methods used in commercial EDA placers, and more naturally handles utilization (cf. the cell_area_utilization inflation parameter in CT-Grouping) [31].

REFERENCES

- [1] A. Agnesina, P. Rajvanshi, T. Yang et al., “AutoDMP: Automated DREAMPlace-based Macro Placement”, *Proc. ISPD*, 2023.
- [2] T. Ajayi, V. A. Chhabria, M. Fogaça et al., “Toward an Open-Source Digital Flow: First Learnings from the OpenROAD Project”, *Proc. ACM/IEEE DAC*, 2019, pp. 76:1-76:4.
- [3] C.-K. Cheng, A. B. Kahng, I. Kang and L. Wang, “RePLAce: Advancing Solution Quality and Routability Validation in Global Placement”, *IEEE TCAD* 38(9) (2018), pp. 1717-1730.
- [4] A. B. Kahng, M. Kim, S. Kim and M. Woo, “RosettaStone: Connecting the Past, Present and Future of Physical Design Research”, *IEEE Design & Test*, 2022.
- [5] A. B. Kahng, “AI system outperforms humans in designing floorplans for microchips”, *Nature News and Views*, 2021. <https://www.nature.com/articles/d41586-021-01515-9>
- [6] Y. Lin, Z. Jiang, J. Gu et al., “DREAMPlace: Deep Learning Toolkit-Enabled GPU Acceleration for Modern VLSI Placement”, *IEEE TCAD* 40(4) (2021), pp. 748-761.
- [7] Y. Lin, W. Li, J. Gu et al., “ABCDPlace: Accelerated Batch-Based Concurrent Detailed Placement on Multithreaded CPUs and GPUs”, *IEEE TCAD* 39(12) (2020), pp. 5083-5096.
- [8] I. L. Markov, J. Hu and M. Kim, “Progress and Challenges in VLSI Placement Research”, *Proc. IEEE* 103(11) (2015), pp. 1985-2003.
- [9] A. Mirhoseini, A. Goldie, M. Yazgan et al., “A Graph Placement Methodology for Fast Chip Design”, *Nature* 594 (2021), pp. 207-212.
- [10] L.-T. Wang, Y.-W. Chang and K.-T. Cheng, *Electronic Design Automation: Synthesis, Verification, and Test*, Morgan Kaufmann, 2009.
- [11] “Stronger Baselines for Evaluating Deep Reinforcement Learning in Chip Placement”, August, 2022. <https://statmodeling.stat.columbia.edu/wp-content/uploads/2022/05/MLcontra.pdf>
- [12] D. Junkin, “Supporting the Scientific Method for the Next Generation of Innovators”, DAC-2022 BoF *Open-Source EDA and Benchmarking Summit*. <https://bit.ly/3kK60jB>
- [13] Ariane RISC-V CPU Repo. <https://github.com/openhwgroup/cva6>
- [14] BlackParrot Repo. <https://github.com/black-parrot/black-parrot>
- [15] MemPool Repo. <https://github.com/pulp-platform/mempool>
- [16] NanGate45 PDK. <https://eda.ncsu.edu/freepdk/freepdk45/>
- [17] BSG Black-box SRAM Generator Repo. https://github.com/jjcherry56/bsg_fakeram
- [18] ASAP7 PDK and Cell Libraries Repo. <https://github.com/The-OpenROAD-Project/asap7>
- [19] SkyWater Open Source PDK. <https://github.com/google/skywater-pdk>
- [20] FakeRAM2.0 Repo. <https://github.com/ABKGroup/FakeRAM2.0>
- [21] ICCAD04 Mixed-size Placement Benchmarks. <http://vlsicad.eecs.umich.edu/BK/ICCAD04bench/>
- [22] RePLAce Repo. <https://github.com/mgwoo/RePLAce>, *commit hash: f500065*.
- [23] Circuit Training: An Open-source Framework for Generating Chip Floorplans with Distributed Deep Reinforcement Learning. https://github.com/google-research/circuit_training, *commit hash: 91e14fd1ca*.
- [24] Circuit Training: An Open-source Framework for Generating Chip Floorplans with Distributed Deep Reinforcement Learning. https://github.com/google-research/circuit_training, *commit hash: 8c6925f2ce*.
- [25] NVDLA Open Source Hardware. https://github.com/nvdlahw/tree/nv_small
- [26] NTUplace3 detailed placer. <http://eda.ee.ntu.edu.tw/research.htm>
- [27] G. Wu, Google Brain, *personal communication*, August 2022.
- [28] J. Jung, *personal communication*, December 2022.
- [29] P. Haspel and A. Hwang, *personal communication*, December 2022.
- [30] M. Cavalcante and J. Liu, *personal communication*, December 2022.
- [31] J. Jiang, Google Brain, *personal communication*, January 2023.
- [32] RePLAce in OpenROAD. <https://bit.ly/3DxpoH5>
- [33] MacroPlacement Repo. <https://github.com/TILOs-AI-Institute/MacroPlacement>
- [34] Our Progress: A Chronology. <http://bit.ly/3kTHJHT>
- [35] Implementation of Proxy Cost Computation. <https://bit.ly/3XNkcHh>
- [36] Implementation of Simulated Annealing. <https://bit.ly/3jg3Yam>
- [37] A. B. Kahng, “For the Record” and Updates, June 2022 - present. <https://bit.ly/3Hl3mYW>
- [38] Impact of initial placement on the outcome of CT. <https://bit.ly/3kzg8LO>
- [39] Implementation of force-directed placement. <https://bit.ly/3Hgx29T>
- [40] MacroPlacement testcases. <https://bit.ly/3RcPl4b>
- [41] SKY130HD FakeStack. <https://bit.ly/403vdpH>
- [42] MacroPlacement tool flow scripts. <https://bit.ly/3WVbxBn>
- [43] Macro shuffling experiment results. <https://bit.ly/3XIBFjR>
- [44] Proxy cost correlation with post-RouteOpt metrics. <https://bit.ly/3DIOD9B>
- [45] Assumptions for power delivery network. <https://bit.ly/3RiHr9m>
- [46] Power delivery network script. <https://bit.ly/3DC6df0>
- [47] Comparison of UCSD proxy cost evaluation with CT binary. <https://bit.ly/3HlJoNZ>
- [48] Effect of different physical synthesis tool on CT solution. <https://bit.ly/3wIAftM>
- [49] Ariane-NG45 CT result generated by Google engineers. <https://bit.ly/3Rgi5sV>
- [50] ICCAD04 Testcases: Bookshelf to Protobuf, CT Flow and Results. <https://bit.ly/3wskk2O>